

Article

The Design of Sulfated Ce/HZSM-5 for Catalytic Decomposition of CF₄

Xie Zheng ^{1,2}, Shijie Chen ^{1,2}, Wanning Liu ^{1,2}, Kaisong Xiang ^{2,3,*} and Hui Liu ^{1,2}

¹ School of Metallurgy and Environment, Central South University, Changsha 410083, China; zhengxie@csu.edu.cn (X.Z.); csj19940415@163.com (S.C.); liuwanning@csu.edu.cn (W.L.); leolau@csu.edu.cn (H.L.)

² Chinese National Engineering Research Center for Control & Treatment of Heavy Metal Pollution, Changsha 410083, China

³ School of Chemistry and Chemical Engineering, Central South University, Changsha 410083, China

* Correspondence: xiangkaisong@hotmail.com; Tel.: +86-731-88830875; Fax: +86-731-88710171

Abstract: CF₄ has a global warming potential of 6500 and possesses a lifetime of 50,000 years. In this study, we modified the HZSM-5 catalyst with Ce and sulfuric acid treatment. The S/Ce/HZSM-5 catalyst achieves 41% of CF₄ conversion at 500 °C, which is four times higher than that over Ce/HZSM-5, while the HZSM-5 exhibits no catalytic activity. The effects of modification were studied by using NH₃-TPD, FT-IR of pyridine adsorption, and XPS methods. The results indicated that the modification, especially the sulfuric acid treatment, strongly increased the Lewis acidic sites, strong acidic sites, and moderate acidic sites on catalysts, which are the main active centers for CF₄ decomposition. The mechanism of acidic sites increases by modification and CF₄ decomposition is clarified. The results of this work will help the development of more effective catalysts for CF₄ decomposition.

Keywords: CF₄; perfluorocompounds; catalytic decomposition; Lewis acid site; cerium; sulfuric acid treatment



Citation: Zheng, X.; Chen, S.; Liu, W.; Xiang, K.; Liu, H. The Design of Sulfated Ce/HZSM-5 for Catalytic Decomposition of CF₄. *Polymers* **2022**, *14*, 2717. <https://doi.org/10.3390/polym14132717>

Academic Editor: Giulio Malucelli

Received: 7 June 2022

Accepted: 30 June 2022

Published: 2 July 2022

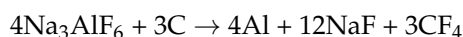
Publisher's Note: MDPI stays neutral with regard to jurisdictional claims in published maps and institutional affiliations.



Copyright: © 2022 by the authors. Licensee MDPI, Basel, Switzerland. This article is an open access article distributed under the terms and conditions of the Creative Commons Attribution (CC BY) license (<https://creativecommons.org/licenses/by/4.0/>).

1. Introduction

Perfluorocarbon (PFC) is a class of greenhouse-gas (GHG) in which all valences of carbon are satisfied with fluorine atoms [1,2]. CF₄ is considered as the most abundant and harmful in PFCs, and it has a high global warming potential, which is about 6500 times higher than that of CO₂ over a 100-year time scale [3]. Due to its symmetry and strong ionic character in the C–F covalent bond, which is the strongest bond (543 kJ mol^{−1}) in organic chemistry, the CF₄ molecule is extremely stable [4]. The aluminum production industry is considered as the main source of CF₄ emission. When the anode effect occurs in the electrolytic cell, the flux Na₃AlF₆ will react with the C anode to form CF₄ as in the equation below [5]. In 2018, the global CF₄ emission from aluminum production is 4.408 Gg, accounting for approximately 4% of total GHG emission in CO₂ equivalent [6]. However, the lifetime of CF₄ in atmosphere is 50,000 years while that of CO₂ is only 10–20 years. Therefore, it is necessary and important to remove CF₄ presented in the exhaust flue gas from the aluminum production industry.



To date, several methods have been developed for CF₄ abatement, such as fueled combustion, plasma, and catalytic hydrolytic decomposition [7–9]. Among them, the catalytic hydrolytic decomposition is considered as the ideal method for its high efficiency and mild reaction temperature compared to others.

HZSM-5 is a molecular sieve catalyst with Si, Al, and O elements as the framework, it has displayed excellent performance in chlorofluorocarbon and hydrofluorocarbon decomposition [10–13]. The catalytic behavior is related to its high specific surface area, strong acidity, and three-dimensional channel system. However, the amount of strong acidic sites and Lewis acidic sites are insufficient for CF₄ decomposition.

Cerium (Ce) is a good promoter for catalyst, due to its high oxygen-storage capacity, high oxygen-vacancy concentration, and the facile Ce⁴⁺/Ce³⁺ redox cycle, which enhances the electron transfer that generates more acidic sites [14,15]. For example, de Rivas et al. [12] studied the 1,2-dichloroethane decomposition over the Ce/HZSM-5 catalyst, and they achieved a 90% conversion that was attributed to the addition of Ce which increased the Lewis acidic sites. Chen et al. [16] synthesized a [Ce-(1,3,5-benzenetricarboxylic acid)(H₂O)₆] catalyst, and achieved a good activity for toluene oxidation with conversion of T_{90%} at 223 °C, the authors concluded that the catalytic activity was due to the great amount of acidic sites on catalyst. Moreover, some research suggests that the sulfuric acid treatment is an excellent strategy to significantly increase the Lewis acidic sites on catalysts, as the sulfate ions act as Lewis acidic sites; meanwhile, they attracted electrons to create more new acidic sites [17,18]. Song et al. [19] modified the γ -Al₂O₃ with Ce and sulfuric acid treatment for CF₄ catalytic decomposition, and found that the addition of Ce increased the acidic sites, the sulfuric acid treatment further enhanced the increasement, and the CF₄ conversions were consistent with the amount of acidic sites. Although varied Lewis acid type catalysts can be applied in CF₄ decomposition, a high temperature (over 700 °C) is required to decompose the CF₄ molecule [20–22]. Therefore, we focused on developing a HZSM-5 based catalyst by modification with element Ce and sulfuric acid treatment for CF₄ decomposition below 700 °C.

Given the above reasons, a series of modified HZSM-5 catalysts were developed to hydrolytic decompose CF₄ at 500 °C. The aim of this work is to investigate the changes in the properties of the catalyst on the addition of Ce and acid treatment. The physicochemical properties of catalysts were characterized by different techniques. This study intended to elucidate the mechanisms of CF₄ decomposition over HZSM-5 based catalysts.

2. Experimental Section

2.1. Catalyst Preparation

The Ce/HZSM-5 catalyst was prepared using the impregnation–calcination method from the commercial molecular sieve HZSM-5 (Si/Al = 18, mole ratio, Nankai Univ, Tianjin, China) calcined at 650 °C in N₂ atmosphere for 5 h with an aqueous solution containing required amounts of cerium nitrate (Sinopharm Chemical Reagent Co., Ltd., Shanghai, China), followed by drying overnight at 80 °C. The Ce/HZSM-5 (10%Ce/HZSM-5) catalyst was crushed and sieved into 60–80 mesh. The Ce/HZSM-5 catalyst was impregnated with an aqueous solution containing H₂SO₄ (98%, Sinopharm Chemical Reagent Co., Ltd., Shanghai, China) under stirring for 24 h and dry for 12 h at 60 °C, the impregnating solution was adjusted to yield the same SO₄²⁻ (12 wt%) as S/Ce/HZSM-5, finally, calcined at 650 °C for 5 h in N₂ atmosphere. The S/Ce/HZSM-5 (12%S/10%Ce/HZSM-5) catalyst was crushed and sieved into 60–80 mesh.

2.2. Catalytic Activity Test

The hydrolytic decomposition of CF₄ was carried out in a fixed-bed reactor. The temperature was maintained at 500 °C. In the aluminum production, the CF₄ generated in electrolytic cell during the anode effect, the CF₄ concentration in the flue gas is about 1%. Therefore, the gas flow consists of 1% CF₄, 35% H₂O, and balanced by Ar. The water was pre-heated at 150 °C and then constantly introduced into the reaction system by using a syringe pump. The effluent gas was washed by aqueous potassium hydroxide to remove the produced HF, and then passed through a cold trap to remove water. Finally, the gas was analyzed by an online gas chromatography (GC-9790 II) equipped with a thermal conductivity detector (TCD).

2.3. Catalyst Characterization

The morphology of the samples was examined by scanning electron microscope (SEM, JSM-IT300LA, JEOL, Tokyo, Japan) with energy dispersive X-ray (EDX) analysis. The X-ray diffraction analysis was performed on a TTR III diffractometer (XRD, Rigaku, Tokyo, Japan). The chemical composition and state of the elements on catalyst surfaces were investigated by X-ray photoelectron spectroscopy (XPS, EscaLab 250Xi, Thermo Fisher, Waltham, MA, USA). The specific surface areas were measured with the N₂ adsorption method on an ASAP analyzer (BET, ASAP2020, Micromeritics, Norcross, GA, USA). Ammonia temperature programmed desorption (NH₃-TPD, AutoChem II 2920, Micromeritics, Norcross, GA, USA) analyses were performed using the following procedures. A 100 mg sample was pretreated at 550 °C, with helium flow of 30 mL/min for 1 h, and then cooled to 50 °C. Ammonia (10% NH₃/He) was introduced to the catalyst for 1 h at 50 °C. After that, the sample was flushed with helium of 50 mL/min for 1 h to remove absorbed NH₃, then the temperature was programmed to increase to 900 °C at a rate of 10 °C/min. The amount of ammonia desorbed from the catalyst was detected using TCD. Fourier transform infrared spectra (FT-IR, Nicolet iS50, Thermo Fisher, Waltham, MA, USA) of pyridine absorption were conducted using the following procedures. The sample was pressed and put into an IR cell, and then it was degassed at 400 °C under vacuum for 2 h to dehydrate. Next, the cell was cooled to room temperature, and the background signal was recorded. After that, pyridine vapor was introduced to the system until reaching adsorption equilibrium. The sample was evacuated out at 150 °C for 30 min followed by cooling down to 50 °C, and then spectral acquisition was performed.

3. Results and Discussion

3.1. Characterization of Catalysts

The morphology and elemental distribution of catalysts were monitored by SEM and EDS mapping, as shown in Figure 1. The microscopic images of HZSM-5 (Figure 1A) exhibit the nano-blocky particles with a smooth surface. The modified catalyst Ce/HZSM-5 (Figure 1B) and the S/Ce/HZSM-5 (Figure 1C,D) exhibit rough surface, the catalysts were covered by small solid granule. The EDS mapping for S/Ce/HZSM-5 (Figure 1E–I) exhibits the uniform distribution of O, Si, Al, S and Ce, respectively.

The X-ray diffraction (XRD) was performed to investigate the crystal structure of the catalysts as in Figure 2. All the samples contain the HZSM-5 [23], and the peak of CeO₂ (JCPDS:34-0394) is observed in modified samples, indicating the formation of CeO₂ [24]. It should be noted that the peak of Ce₂(SO₄)₃ is not observed in the S/Ce/HZSM-5 catalyst, which indicated the absence of reaction between Ce and sulfuric acid during the catalyst preparation step. The specific surface area and pore diameter of catalysts were analyzed, as listed in Table 1. The surface area of catalysts decreased from 248 m² g⁻¹ to 148 m² g⁻¹, and the pore diameter decreased from 2.38 nm to 2.28 nm after modified by Ce, these changes are in agreement with previous research [19,25], which may account for the formation of CeO₂ on the surface of catalysts, in addition to element Ce, some cation ions were replaced by Ce, the CeO₂ would block the original pore, results in the surface area and pore diameter decreasing. The surface area and pore diameter increased to 278 m² g⁻¹ and 2.28 nm, respectively, after the sulfate acid treatment. This may be due to the fact that acid treatment increased the amount of amorphous silica [26].

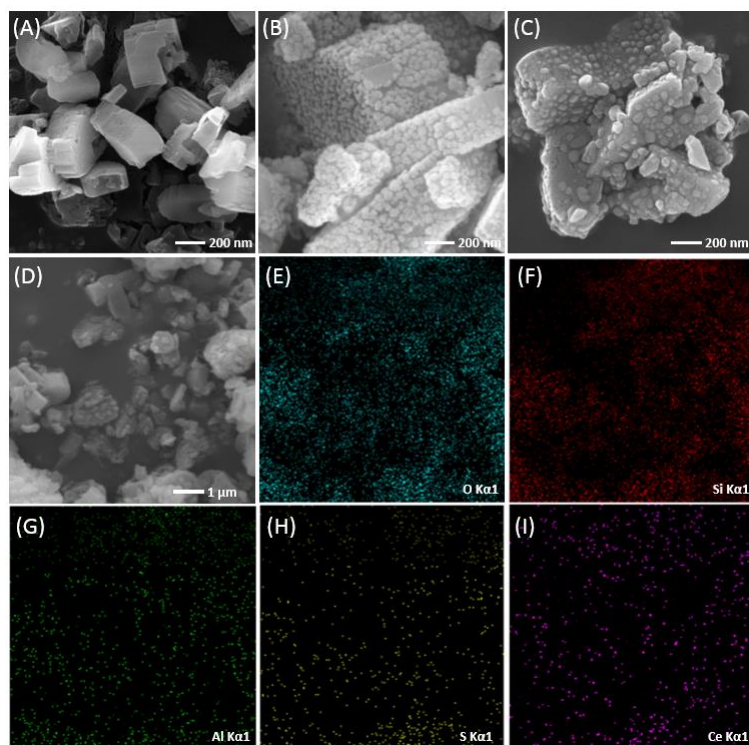


Figure 1. SEM of (A) HZSM-5, (B) Ce/HZSM-5, (C,D) S/Ce/HZSM-5, and SEM-EDS mapping for S/Ce/HZSM-5 (E–I).

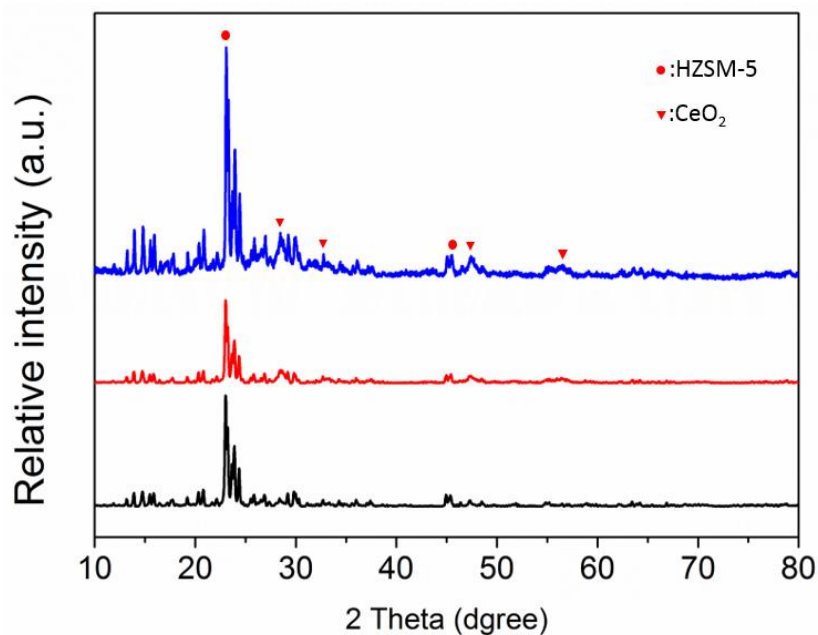


Figure 2. X-ray diffraction (XRD) patterns of the catalysts, (1) HZSM-5, (2) Ce/HZSM-5, and (3) S/Ce/HZSM-5.

Table 1. Specific surface area, pore diameter for the catalysts.

Catalysts	BET Surface Area ($\text{m}^2 \text{g}^{-1}$)	Pore Diameter (nm)
HZSM-5	248	2.38
Ce/HZSM-5	148	2.28
S/Ce/HZSM-5	278	2.63

The NH₃-TPD experiments were conducted to analyze the different kinds of acidic sites in the catalysts. There are three kinds of acidic site according to the desorption temperature of NH₃ on catalysts: weak acidic sites ($T < 250$ °C), moderate acidic sites (250 °C $< T < 600$ °C), and strong acidic sites ($T > 600$ °C) [27–29]. The TPD results are shown in Figure 3 and Table 2, the HZSM-5 catalyst exhibited the most weak acidic sites ($663 \mu\text{mol g}^{-1}$) and the second highest amount of moderate acidic sites ($267 \mu\text{mol g}^{-1}$), the strong acidic site was not observed. The addition of Ce decreased the amount of weak acidic sites to $290 \mu\text{mol g}^{-1}$ and increased the moderate acidic sites to $544 \mu\text{mol g}^{-1}$, but still, no strong acidic site was observed. After further acid treatment, the amount of weak acidic sites decreased to $273 \mu\text{mol g}^{-1}$ and the amount of moderate acidic sites increased to $855 \mu\text{mol g}^{-1}$, the amount of strong acidic sites dramatically increased to $1274 \mu\text{mol g}^{-1}$, which dominated over others. These findings strongly indicated that the impregnation with sulfate group influenced the acidic properties of catalysts, the amount of moderate and strong acidic sites significantly increased; moreover, the ratio of (strong + moderate)/weak was in the following order: S/Ce/HZSM-5(7.80) $>$ Ce/HZSM-5(1.88) $>$ HZSM-5(0.40).

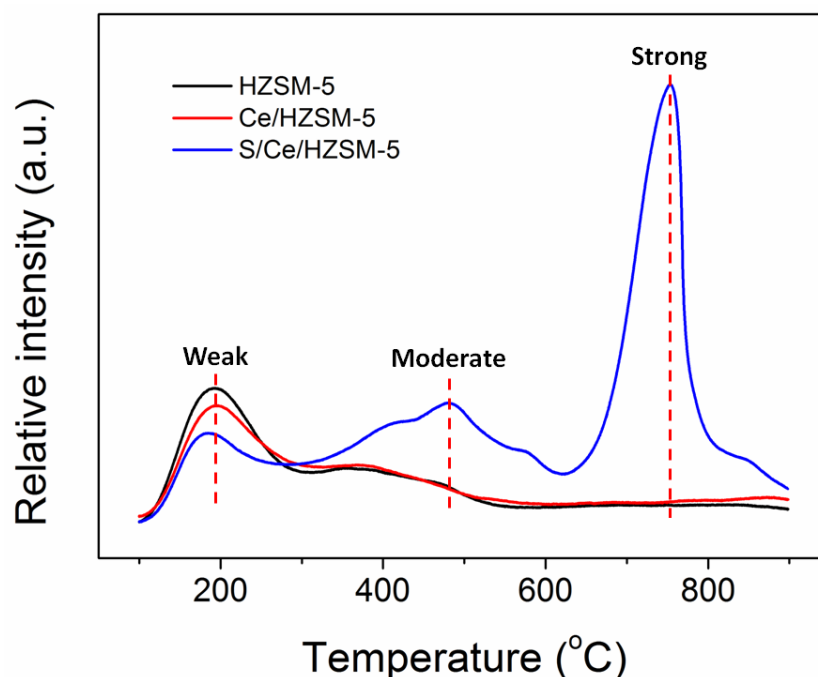


Figure 3. NH₃-TPD profiles of catalysts.

Table 2. NH₃-TPD acidic sites results for the catalyst.

Catalysts	Amount of Acid Site ($\mu\text{mol g}^{-1}$)				
	Weak	Moderate	Strong	Total	(Strong + Moderate)/Weak
HZSM-5	663	267	0	930	0.40
Ce/HZSM-5	290	544	0	834	1.88
S/Ce/HZSM-5	273	855	1274	2402	7.80

In order to gain more information on acidic properties of catalysts, the FT-IR spectra of pyridine adsorption experiments are conducted as shown in Figure 4 and Table 3. The spectra are recorded over a frequency range from 1400 cm^{-1} to 1700 cm^{-1} , where characteristic vibration modes of adsorbed pyridine will appear. According to the references [30,31], the characteristic wave number of 1455 cm^{-1} , 1612 cm^{-1} could be assigned to the pyridine species coordinatively adsorbed on Lewis acid sites, while the wave number of 1545 cm^{-1} , 1635 cm^{-1} assigned to pyridinium ion formed on Brønsted acid sites, the 1490 cm^{-1} peak was attributable to the L+B acid sites. The amounts of L-acid site on HZSM-5, Ce/HZSM-5 and

S/Ce/HZSM-5 were $120.57 \mu\text{mol g}^{-1}$, $138.26 \mu\text{mol g}^{-1}$ and $156.84 \mu\text{mol g}^{-1}$, respectively. The amount of Brønsted acid sites showed the reversed trend, they were $233.91 \mu\text{mol g}^{-1}$, $83.61 \mu\text{mol g}^{-1}$ and $69.97 \mu\text{mol g}^{-1}$, respectively. The ratio of Lewis/Brønsted was in the following order: S/Ce/HZSM-5(2.24) > Ce/HZSM-5(1.65) > HZSM-5(0.52). The results indicated that the addition of Ce increased the amount of Lewis acidic sites while decreasing the Brønsted acidic sites; furthermore, the acid treatment enhanced the influence.

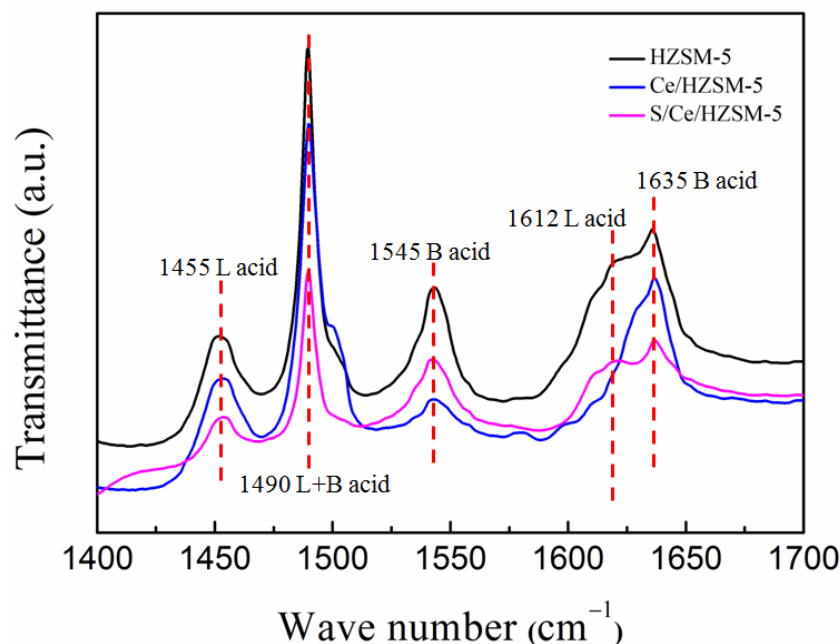


Figure 4. FT-IR spectra of pyridine adsorption on catalysts.

Table 3. FT-IR spectra of pyridine adsorption results for the catalyst.

Catalysts	Amount of Acid Site ($\mu\text{mol g}^{-1}$)		
	L-Acid Site	B-Acid Site	Lewis/Brønsted (L/B)
HZSM-5	120.57	233.91	0.52
Ce/HZSM-5	138.26	83.61	1.65
S/Ce/HZSM-5	156.84	69.97	2.24

3.2. Catalytic Performance of CF_4 Decomposition

The conversion reactions of CF_4 over catalysts were conducted at different temperature, as shown in Figure 5. The HZSM-5 exhibited no catalytic activity below 600°C , and only 14% conversion of CF_4 while the temperature increased up to 700°C . The Ce/HZSM-5 exhibited a higher CF_4 conversion compared to HZSM-5, the CF_4 conversions at 500°C , 550°C , 600°C , 650°C and 700°C were 10%, 41%, 52%, 60% and 63%, respectively. As for the S/Ce/HZSM-5 catalyst, the CF_4 conversion was further enhanced, they were 41%, 50%, 63%, 66% and 67%, respectively. Moreover, at the temperature of 500°C , the conversion of S/Ce/HZSM-5 was four times higher than that of Ce/HZSM-5. These results indicated that the acid treatment significantly increased the catalytic activity of Ce/HZSM-5, which showed a good agreement with the results of BET, NH_3 -TPD and FT-IR.

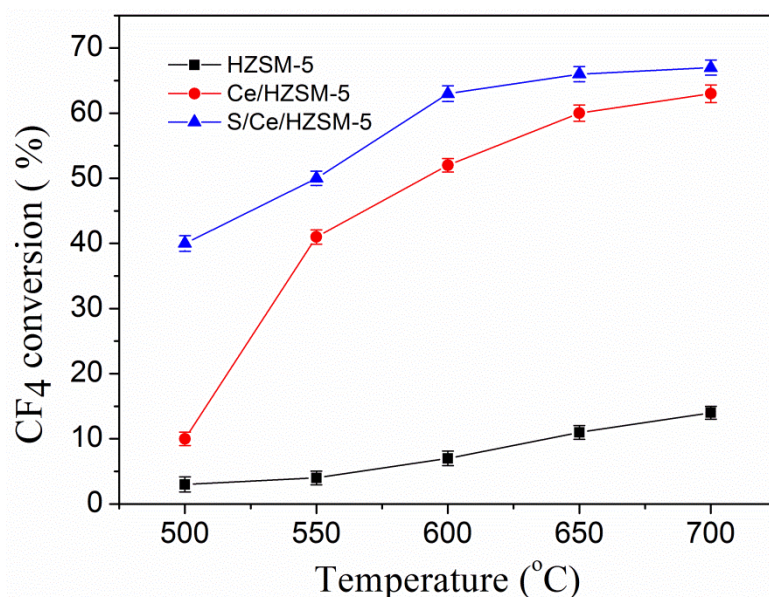


Figure 5. CF₄ conversion reaction over catalysts at different temperatures.

The stability of catalysts was tested for 60 h at 500 °C as shown in Figure 6. The CF₄ conversion over S/Ce/HZSM-5 decreased from 41% to 34% (17% loss), while the conversion over Ce/HZSM-5 decreased from 11% to 7% (27% loss). The catalytic stability of S/Ce/HZSM-5 was much higher than that of Ce/HZSM-5. This may be due to the increment of acidic sites by acid treatment.

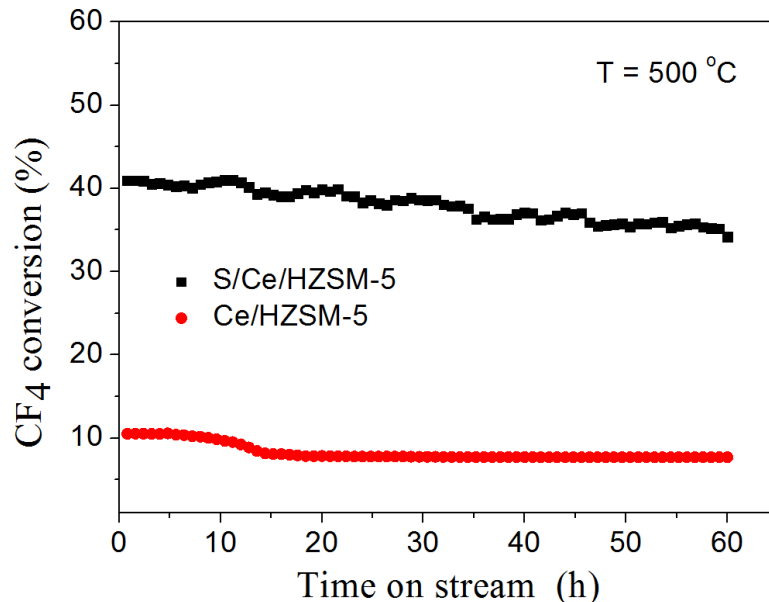


Figure 6. CF₄ conversion over catalysts with time on stream.

3.3. Mechanism Analysis of Hydrolytic Decomposition of CF₄

In order to demonstrate the main factor that promoted the catalytic activity of catalysts, the close correlation between CF₄ conversion and the ratio of (strong + moderate)/weak and Lewis/Brønsted were performed as shown in Figure 7. The correlation showed that the conversion is related to the ratio of (strong + moderate)/weak and the ratio of Lewis/Brønsted. Therefore, we concluded that the strong + moderate acidic sites and the Lewis acidic sites, are the main factor that promoted the activity of the catalysts. The HZSM-5 exhibited no catalytic activity due to its low ratio of (strong + moderate)/weak and Lewis/Brønsted.

Similarly, it has been reported that the Lewis acid sites and strong + moderate acid sites played a promoting role in the decomposition of hydrofluorocarbons [32–34]. The results strongly suggest that the direct participation of the acid sites in CF_4 decomposition is probably a step for subtracting fluorine atom from CF_4 molecule by Lewis acid sites. The addition of element Ce and the acid treatment could significantly influence the acidic property, resulting in increasing the catalytic activity and stability of catalysts in CF_4 decomposition.

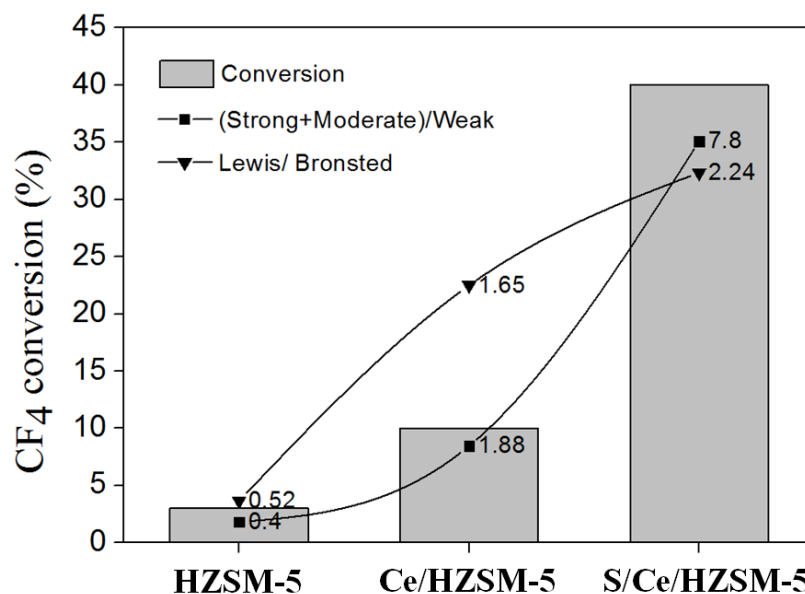


Figure 7. Correlation between CF_4 conversion and ratio of (strong + moderate)/weak and Lewis/Bronsted.

In order to acquire insights into the surface chemical composition of catalysts, X-ray photoelectron spectroscopy (XPS) analysis of catalysts was carried out and shown in Figure 8 and Table 4. A curve-fitting for this analysis was carried out after Shirley-type background subtraction using a combination of Gaussian and Lorentzian functions. Figure 8A presented the S 2p core level spectra, the two major binding energy values were located at 168.90 eV and 170.10 eV, attributing to S 2p_{1/2} and S 2p_{2/3} respectively, which were ascribed to S⁶⁺ from SO₄²⁻. According to references [17,18,35], the S⁶⁺ from SO₄²⁻ could significantly increase the amount of Lewis acidic sites, which showed a good agreement with the results of NH₃-TPD and FT-IR. The O 1s core level spectra of catalysts were shown in Figure 8B, there are three major binding energy values located at range 528.9 to 529.5 eV, range 530.0 to 531.6 eV, and range 531.9 to 533.2 eV, attributing to O_{lat}, O_{sur} and O_{ads}, respectively [36,37]. After the acid treatment, the peak of O_{lat} disappeared, the intensity of peak for O_{ads} increased, it could be concluded that the O_{lat} were transformed to O_{ads}, meanwhile, some of the O_{lat} bonded with S⁶⁺ to form SO₄²⁻, then increased the amount of Lewis acidic sites. The Ce 3d core level spectra of catalysts are shown in Figure 8C, the peak v₂ (885.9 eV–886.3 eV) and peak u₂ (904.0 eV–904.5 eV) were ascribed to Ce³⁺, the peak v₁ (883.0 eV), peak v₃ (887.3 eV–889.1 eV), peak v₄ (898.8 eV), peak u₁ (901.5 eV), peak u₃ (905.9 eV–907.7 eV) and peak u₄ (917.3 eV) were ascribed to Ce⁴⁺ [38,39], after the sulfuric acid treatment, the peak u₄ and peak v₄ disappeared, the Ce³⁺/Ce increased from 25.9% to 31.0%, indicating that the sulfuric acid treatment reduced the Ce⁴⁺ to Ce³⁺ because they attracted electrons to create more Lewis acidic sites, which showed a good agreement with the CF_4 conversion performance and the results of NH₃-TPD and FT-IR.

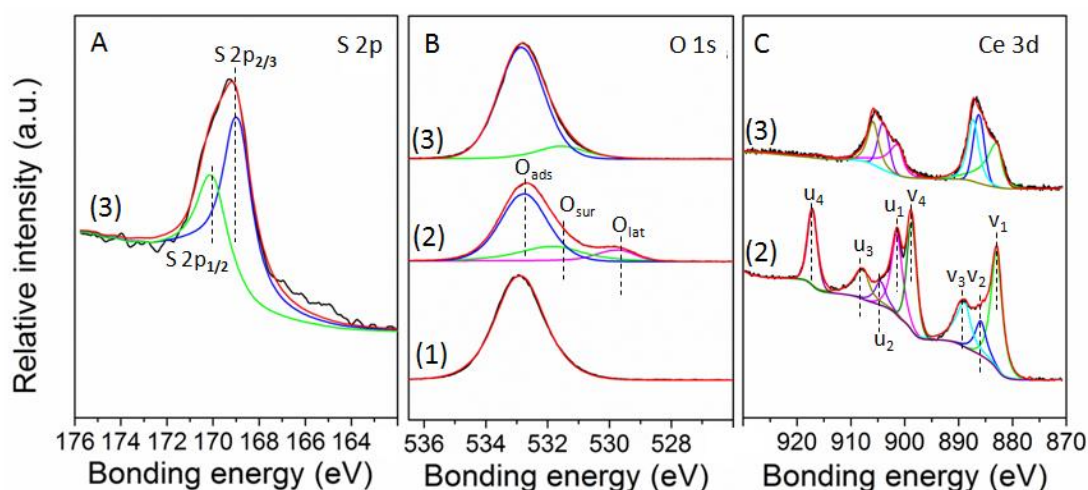


Figure 8. X-ray photo electron spectroscopy (XPS) spectra of catalyst, (A): S 2p for catalyst, (B): O 1s for catalysts, and (C): Ce 3d for catalysts. (1) HZSM-5, (2) Ce/HZSM-5, and (3) S/Ce/HZSM-5.

Table 4. Surface atomic distribution of element O and Ce.

Catalysts	Distribution (%)			
	O _{lat}	O _{sur}	O _{ads}	Ce ³⁺ /Ce
HZSM-5	0	0	100	/
Ce/HZSM-5	10.5	22.0	67.5	25.9
S/Ce/HZSM-5	0	10.1	89.9	31.0

4. Conclusions

We modified the commercial HZSM-5 with the addition of Ce (Ce/HZSM-5) and further sulfuric acid treatment (S/Ce/HZSM-5). The S/Ce/HZSM-5 catalyst achieved a 41% CF₄ conversion at 500 °C which is four times higher than that over Ce/HZSM-5, while the HZSM-5 exhibited no catalytic activity. The close correlation between CF₄ catalytic conversion and acidic property indicated that the Lewis acidic sites and moderate + strong acidic sites are the main factors that promoted the activity of the catalysts. The effects of modification were confirmed by using NH₃-TPD, FT-IR of pyridine adsorption and XPS methods. These results indicate that the acidity properties of catalysts are strongly influenced by the addition of Ce and further sulfuric acid treatment, and then significantly improved the catalytic activity in the CF₄ decomposition process, which is an acid-catalyzed reaction.

Author Contributions: All authors contributed to the study conception and design, X.Z., S.C. and W.L. developed and designed the methodology of this experiment. X.Z. prepared the original draft and K.X. revised the manuscript. H.L. supervised the project and had leadership responsibility for the research. All authors have read and agreed to the published version of the manuscript.

Funding: This work was financially supported by National Natural Science Foundation of China (51974378), Innovative Research Group Project of the National Natural Science Foundation of China (52121004) and Special Funding for Innovative Province Construction of Hunan (2019RS3006).

Institutional Review Board Statement: Not applicable.

Informed Consent Statement: Not applicable.

Data Availability Statement: The data supporting this study are available from the corresponding author upon reasonable request.

Conflicts of Interest: The authors declare no competing interest.

References

1. O'Hagan, D. Understanding organofluorine chemistry. An introduction to the C–F bond. *Chem. Soc. Rev.* **2008**, *37*, 308–319. [CrossRef] [PubMed]
2. Hannus, I. Adsorption and transformation of halogenated hydrocarbons over zeolites. *Appl. Catal. A Gen.* **1999**, *189*, 263–276. [CrossRef]
3. Mühle, J.; Ganesan, A.L.; Miller, B.R.; Salameh, P.K.; Harth, C.M.; Grealley, B.R.; Rigby, M.; Porter, L.W.; Steele, L.P.; Trudinger, C.M.; et al. Perfluorocarbons in the global atmosphere: Tetrafluoromethane, hexafluoroethane, and octafluoropropane. *Atmos. Chem. Phys.* **2010**, *10*, 5145–5164. [CrossRef]
4. Tsai, W.T.; Chen, H.P.; Hsien, W.Y. A review of uses, environmental hazards and recovery/recycle technologies of perfluorocarbons (PFCs) emissions from the semiconductor manufacturing processes. *J. Loss Prevent. Proc. Ind.* **2002**, *15*, 65–75. [CrossRef]
5. Tabereaux, A.T. Anode effects, PFCs, global warming, and the aluminum industry. *J. Miner. Met. Mater. Soc. (TMS)* **1994**, *46*, 30–34. [CrossRef]
6. Perfluorocarbon (PFC) Emissions—International Aluminium Institute. Available online: <https://international-aluminium.org/> (accessed on 5 June 2022).
7. Zheng, X.; Zheng, X.; Xiang, K.; Shen, F.; Liu, H. The Zr Modified γ -Al₂O₃ Catalysts for Stable Hydrolytic Decomposition of CF₄ at Low Temperature. *Catalysts* **2022**, *12*, 313. [CrossRef]
8. Jia, L.; Ma, S. The Experimental Study on High Temperature Air Combustion and CF₄ Decomposition. In Proceedings of the Heat Transfer Summer Conference, San Francisco, CA, USA, 17–22 July 2005; pp. 705–708.
9. Efremov, A.; Lee, J.; Kim, J. On the Control of Plasma Parameters and Active Species Kinetics in CF₄/O₂/Ar Gas Mixture by CF₄/O₂ and O₂/Ar Mixing Ratios. *Plasma Chem. Plasma Process.* **2017**, *37*, 1445–1462. [CrossRef]
10. Hou, X.; Qiu, Y.; Yuan, E.; Zhang, X.; Liu, G. SO₄²⁻/TiO₂ promotion on HZSM-5 for catalytic cracking of paraffin. *Appl. Catal. A Gen.* **2017**, *537*, 12–23. [CrossRef]
11. Yang, Z.; Cao, J.P.; Retn, X.Y.; Zhao, X.Y.; Liu, S.N.; Guo, Z.X.; Shen, W.Z.; Bai, J.; Wei, X.Y. Preparation of hierarchical HZSM-5 based sulfated zirconium solid acid catalyst for catalytic upgrading of pyrolysis vapors from lignite pyrolysis. *Fuel* **2019**, *237*, 1079–1085. [CrossRef]
12. de Rivas, B.; Sampedro, C.; Ramos-Fernandez, E.V.; Lopez-Fonseca, R.; Gascon, J.; Makkee, M.; Gutiérrez-Ortiz, J.I. Influence of the synthesis route on the catalytic oxidation of 1,2-dichloroethane over CeO₂/H-ZSM5 catalysts. *Appl. Catal. A Gen.* **2013**, *456*, 96–104. [CrossRef]
13. Joshi, Y.V.; Thomson, K.T. The roles of gallium hydride and Brønsted acidity in light alkane dehydrogenation mechanisms using Ga-exchanged HZSM-5 catalysts: A DFT pathway analysis. *Catal. Today* **2005**, *105*, 106–121. [CrossRef]
14. Zhan, W.; Guo, Y.; Gong, X.; Guo, Y.; Wang, Y. Current status and perspectives of rare earth catalytic materials and catalysis. *Chin. J. Catal.* **2014**, *35*, 1238–1250. [CrossRef]
15. Dai, Q.; Wang, W.; Wang, X.; Lu, W. Sandwich-structured CeO₂@ZSM-5 hybrid composites for catalytic oxidation of 1,2-dichloroethane: An integrated solution to coking and chlorine poisoning deactivation. *Appl. Catal. B Environ.* **2017**, *203*, 31–42. [CrossRef]
16. Chen, X.; Yu, E.; Cai, S.; Jia, H.; Chen, J.; Liang, P. In situ pyrolysis of Ce-MOF to prepare CeO₂ catalyst with obviously improved catalytic performance for toluene combustion. *Chem. Eng. J.* **2018**, *344*, 469–479. [CrossRef]
17. Jia, W.; Wu, Q.; Lang, X.; Hu, C.; Zhao, G.; Li, J.; Zhu, Z. Influence of Lewis Acidity on Catalytic Activity of the Porous Alumina for Dehydrofluorination of 1,1,1,2-Tetrafluoroethane to Trifluoroethylene. *Catal. Lett.* **2015**, *145*, 654–661. [CrossRef]
18. Mekhemer, G.A.H.; Khalaf, H.A.; Mansour, S.A.A.; Nohman, A.K.H. Sulfated Alumina Catalysts: Consequences of Sulfate Content and Source. *Mon. Für Chem./Chem. Mon.* **2005**, *136*, 2007–2016. [CrossRef]
19. Song, J.Y.; Chung, S.H.; Kim, M.S.; Seo, M.G.; Lee, Y.H.; Lee, K.Y.; Kim, J.S. The catalytic decomposition of CF₄ over Ce/Al₂O₃ modified by a cerium sulfate precursor. *J. Mol. Catal. A Chem.* **2013**, *370*, 50–55. [CrossRef]
20. Xu, X.; Jeon, J.Y.; Choi, M.H.; Kim, H.Y.; Choi, W.C.; Park, Y.K. A Strategy to Protect Al₂O₃-based PFC Decomposition Catalyst from Deactivation. *Chem. Lett.* **2005**, *34*, 364–365. [CrossRef]
21. El-Bahy, Z.; Ohnishi, R.; Ichikawa, M. Hydrolysis of CF₄ over alumina-based binary metal oxide catalysts. *Appl. Catal. B Environ.* **2003**, *40*, 81–91. [CrossRef]
22. Takita, Y.; Morita, C.; Ninomiya, M.; Wakamatsu, H.; Nishiguchi, H.; Ishihara, T. Catalytic Decomposition of CF₄ over AlPO₄-Based Catalysts. *Chem. Lett.* **1999**, *28*, 417–418. [CrossRef]
23. Dwivedi, U.; Naik, S.N.; Pant, K.K. High quality liquid fuel production from waste plastics via two-step cracking route in a bottom-up approach using bi-functional Fe/HZSM-5 catalyst. *Waste Manag.* **2021**, *132*, 151–161. [CrossRef] [PubMed]
24. Liu, Y.; Ma, C.; Zhang, Q.; Pan, P.; Gu, L.; Xu, D.; Bao, J.; Dai, Z. 2D Electron Gas and Oxygen Vacancy Induced High Oxygen Evolution Performances for Advanced Co₃O₄/CeO₂ Nanohybrids. *Adv. Mater.* **2019**, *31*, 1900062. [CrossRef] [PubMed]
25. Takita, Y.; Ninomiya, M.; Miyake, H.; Wakamatsu, H.; Yoshinaga, Y.; Ishihara, T. Catalytic decomposition of perfluorocarbons Part II. Decomposition of CF₄ over AlPO₄-rare earth phosphate catalysts. *Phys. Chem. Chem. Phys.* **1999**, *1*, 4501–4504. [CrossRef]
26. Panda, A.K.; Mishra, B.G.; Mishra, D.K.; Singh, R.K. Effect of sulphuric acid treatment on the physico-chemical characteristics of kaolin clay. *Colloids Surf. A Physicochem. Eng. Asp.* **2010**, *363*, 98–104. [CrossRef]
27. Stanculescu, M.; Bulsink, P.; Caravaggio, G.; Nossova, L.; Burich, R. NH₃-TPD-MS study of Ce effect on the surface of Mn- or Fe-exchanged zeolites for selective catalytic reduction of NO_x by ammonia. *Appl. Surf. Sci.* **2014**, *300*, 201–207. [CrossRef]

28. Benaliouche, F.; Boucheffa, Y.; Ayrault, P.; Mignard, S.; Magnoux, P. NH₃-TPD and FTIR spectroscopy of pyridine adsorption studies for characterization of Ag- and Cu-exchanged X zeolites. *Microporous Mesoporous Mater.* **2008**, *111*, 80–88. [[CrossRef](#)]
29. Luo, J.; Kamasamudram, K.; Currier, N.; Yezerets, A. NH₃-TPD methodology for quantifying hydrothermal aging of Cu/SSZ-13 SCR catalysts. *Chem. Eng. Sci.* **2018**, *190*, 60–67. [[CrossRef](#)]
30. Xu, X.; Jeon, J.Y.; Choi, M.H.; Kim, H.Y.; Choi, W.C.; Park, Y.K. The modification and stability of γ -Al₂O₃ based catalysts for hydrolytic decomposition of CF₄. *J. Mol. Catal. A Chem.* **2007**, *266*, 131–138. [[CrossRef](#)]
31. Damyanova, S.; Centeno, M.; Petrov, L.; Grange, P. Fourier transform infrared spectroscopic study of surface acidity by pyridine adsorption on Mo/ZrO₂-SiO₂(Al₂O₃) catalysts. *Spectrochim. Acta Part A Mol. Biomol. Spectrosc.* **2001**, *57*, 2495–2501. [[CrossRef](#)]
32. Takita, Y.; Anabe, T.; Ito, M.; Ogura, M.; Muraya, T.; Yasuda, S.; Nishiguchi, H.; Ishihara, T. Decomposition of CH₂FCF₃ (134a) over Metal Phosphate Catalysts. *Ind. Eng. Chem. Res.* **2002**, *41*, 2585–2590. [[CrossRef](#)]
33. Swamidoss, C.M.A.; Sheraz, M.; Anus, A.; Jeong, S.; Park, Y.-K.; Kim, Y.-M.; Kim, S. Effect of Mg/Al₂O₃ and Calcination Temperature on the Catalytic Decomposition of HFC-134a. *Catalysts* **2019**, *9*, 270. [[CrossRef](#)]
34. Takita, Y.; Moriyama, J.-I.; Nishiguchi, H.; Ishihara, T.; Hayano, F.; Nakajo, T. Decomposition of CCl₂F₂ over metal sulfate catalysts. *Catal. Today* **2004**, *88*, 103–109. [[CrossRef](#)]
35. Wang, T.; Liu, H.; Zhang, X.; Liu, J.; Zhang, Y.; Guo, Y.; Sun, B. Catalytic conversion of NO assisted by plasma over Mn-Ce/ZSM5-multi-walled carbon nanotubes composites: Investigation of acidity, activity and stability of catalyst in the synergic system. *Appl. Surf. Sci.* **2018**, *457*, 187–199. [[CrossRef](#)]
36. Zhao, H.; Zhao, H.; Han, W.; Dong, F.; Tang, Z. Enhanced catalytic performance of Nb doping Ce supported on ordered mesoporous TiO₂-SiO₂ catalysts for catalytic elimination of 1,2-dichlorobenzene. *Mol. Catal.* **2019**, *479*, 110638. [[CrossRef](#)]
37. Liu, B.; Li, C.; Zhang, G.; Yao, X.; Chuang, S.S.C.; Li, Z. Oxygen Vacancy Promoting Dimethyl Carbonate Synthesis from CO₂ and Methanol over Zr-Doped CeO₂ Nanorods. *ACS Catal.* **2018**, *8*, 10446–10456. [[CrossRef](#)]
38. Zong, L.; Zhang, G.; Zhao, H.; Zhang, J.; Tang, Z. One pot synthesized CeO₂-WO₃-TiO₂ catalysts with enriched TiO₂ (001) facets for selective catalytic reduction of NO with NH₃ by evaporation-induced self-assembly method. *Chem. Eng. J.* **2018**, *354*, 295–303. [[CrossRef](#)]
39. Han, W.; Zhao, H.; Dong, F.; Tang, Z. Morphology-controlled synthesis of 3D, mesoporous, rosette-like CeCoO_x catalysts by pyrolysis of Ce[Co(CN)₆] and application for the catalytic combustion of toluene. *Nanoscale* **2018**, *10*, 21307–21319. [[CrossRef](#)]